Geochemical Perspectives Letters

Experimental evidence that microbial activity lowers the albedo of glaciers

M. Musilova[1,2]*, M. Tranter[1], J.L. Bamber[1], N. Takeuchi[3], A.M. Anesio[1]

OPEN ACCESS

doi: 10.7185/geochemlet.1611

Abstract

Darkening of glacier and ice sheet surfaces is an important positive feedback to increasing global temperatures. Deposition of impurities on glaciers is primarily believed to reduce surface albedo, resulting in greater melt and mass loss. However, no study has yet included the effects of biological activity in albedo reduction models. Here, we provide the first experimental evidence that microbial activity can significantly decrease glacier surface albedo. Indeed, the addition of nutrients at ice meltwater concentrations to microbe-impurity mixtures resulted in extensive microbial organic carbon fixation and accumulation in Greenland Ice Sheet surface debris. Accumulated organic carbon, over the period of a melt season, darkened the glacial debris in our experiments from 31.1 % to 15.6 % surface reflectivity (used as an analogue for albedo in our calculations), generating a strongly absorbing surface. Our experiments are the first to quantify the microbially-induced potential melt increase for the Greenland Ice Sheet (up to an average of 17.3 ± 2.5 Gt yr^{-1} at present and up to ~85 Gt yr^{-1} by 2100, based on our first order calculations). Mass loss from glaciers will conceivably intensify through enhanced microbial activity, resulting from longer melt seasons and fertilisation from anthropogenic sources.

Received 8 October 2015 | Accepted 27 January 2016 | Published 11 March 2016

Introduction

Glacier surfaces melt primarily by the absorption of solar radiation, which depends on the surface albedo (Boggild *et al.*, 2010; Box *et al.*, 2012). Albedo is affected by the physical properties of snow and ice, such as the geometric pattern of the snow surface (Pirazzini, 2004), snow metamorphism (Nakamura *et al.*, 2001), water content (Ryser *et al.*, 2013) and particulate impurities on the glacier surface (Paterson, 1994). Most studies assume that the accumulation of inorganic and organic particulates, such as anthropogenic and naturally occurring black carbon (Doherty *et al.*, 2013), volcanic ash and dust (Dumont *et al.*, 2014), are key drivers of the darkening and reduction of the ice albedo.

1. Bristol Glaciology Centre, School of Geographical Sciences, University of Bristol, Bristol BS8 1SS, UK
2. Current address: Výskumný ústav potravinársky – NPPC and Slovak Organisation for Space Activities (SOSA), Bratislava, Slovakia
* Corresponding author (email: michaela.musilova@community.isunet.edu)
3. Department of Earth Sciences, Graduate School of Science, Chiba University, 1-33, Yayoicho, Inage-ku, Chiba-city, Chiba, 263-8522, Japan

Recent research shows that there is high microbial activity on glacial surfaces (Anesio *et al.*, 2009), some associated with pigmented algae, which absorb significantly more light than local inorganic dust particles on the Greenland Ice Sheet (GrIS) (Lutz *et al.*, 2014). Furthermore, microbially-rich glacier surface debris (cryoconite) reduces the glacier surface (supraglacial) albedo (Takeuchi *et al.*, 2001). Cryoconite accumulates in water-filled holes on glacier surfaces, causing enhanced melting around the deposited sediment (Fountain *et al.*, 2004). These so-called cryoconite holes contain a substantial amount of organic matter (5–10 %; Takeuchi *et al.*, 2001), with values often >6 % organic carbon (OC) on GrIS (Stibal *et al.*, 2010). Microbial activity is believed to cause a further darkening of the already dark inorganic particulates in cryoconite debris by producing and/or transforming OC (Anesio *et al.*, 2009; Hodson *et al.*, 2010a). Microbes are thought to decompose more labile OC to form dark-coloured humic substances (Takeuchi *et al.*, 2001) and to produce extracellular polymeric substances (EPS) (Hodson *et al.*, 2010b). These glue-like compounds help cement organic and inorganic particles (including black carbon; Stibal *et al.*, 2012a) into granules, thereby increasing their residence time on glacier surfaces (Hodson *et al.*, 2010b; Langford *et al.*, 2010). This can lead to a significant decrease in supraglacial albedo, considering cryoconite debris covers 0.1–10 % of the ablation zone of glaciers in the Northern Hemisphere (Hodson *et al.*, 2007; Anesio *et al.*, 2009; Hodson *et al.*, 2010a).

"We conducted an original laboratory experiment, the 'cryoconite casserole', to investigate the darkening of cryoconite debris as a result of OC accumulation driven by microbial activity. Greenlandic cryoconite debris (10 % natural cryoconite, mixed with 90 % cryoconite furnaced at 550 °C to remove all organic matter) was exposed to simulated Greenlandic summer conditions, in terms of temperature, lighting and nutrient availability (see Methodology in the Supplementary Information for full details). This cryoconite mixture simulated the early stages of cryoconite hole development, where the debris is mostly inorganic and it can become colonised by local microbial communities. Samples were kept either under 'light' (simulated daylight) or 'dark' (covered in aluminium foil) conditions. Three different water/nutrient applications were made: 1) blank, sterile water, 2) nitrogen (N) and phosphorous (P) additions and 3) N, P and organic carbon (C) additions. The nutrient additions simulated concentrations released from ice melt (Stibal *et al.*, 2012b; Telling *et al.*, 2012; Lawson *et al.*, 2014). All light and nutrient treatments had five replicates. Cryoconite casserole samples were analysed for their nutrient composition, surface reflection normal to the ice surface in the laboratory and chlorophyll *a* (chl*a*) concentration. The structure of the debris was observed with an optical and fluorescent microscope. Here, we present data collected at the end of one and three consecutive simulated summer seasons

(the latter was performed to confirm the results observed during the one simulated summer experiment). The reduction of surface reflection due to biological activity, derived from our results, was used as a proxy for a reduction in albedo in the regional climate model Modèle Atmosphérique Régional (MAR; Fettweis *et al.*, 2013) to project future microbially-mediated increases in GrIS melt (see Methodology, Supplementary Information).

Results and Discussion

Supraglacial Microbial Nutrient Production and Recycling. Substantial amounts of OC (~1.7 ± 0.5 mg OC/g of cryoconite) were produced and accumulated by microbes over the course of one simulated summer in 'light' conditions with NPC additions (Fig. 1a), compared to 'dark' and blank samples. OC concentrations quadrupled (~7.0 ± 0.9 mg OC/g of cryoconite) when the samples were exposed to three consecutive simulated summers (Fig. 1b). The total C addition was only 0.25 % of the final accumulated OC. Thus nearly all accumulated OC in this treatment originated from microbial C fixation/transformation.

'Light' treatments with NPC additions also generated the highest concentrations of particulate organic nitrogen (PON; 100.4 ± 26.7 µg PON/g cryoconite) and organic bound phosphorous (OP; 19.5 ± 6.4 µg OP/g cryoconite) (Table 1). By contrast, PON and OP were consumed in the dark NP treatments (6.6 ± 4.4 µg PON/g cryoconite and 22.0 ± 1.7 µg OP/g cryoconite, respectively, after one season). Additionally, the light samples with NPC additions had the biggest decrease in inorganic bound phosphorous (IP; 27.2 ± 5.4 µg IP/g cryoconite consumed), with respect to the starting IP concentrations. This is indicative of an uptake of P from the sediment, as a consequence of microbial fixation of OC. The concentrations of PON and OP increased 7-fold and 4-fold, respectively, for the same samples ('light' with NPC additions) after three simulated summers (Table 1).

The amount of OC produced and accumulated in our experiments simulating glacial surfaces was disproportionate compared to the amounts of C, N and P added to the samples at ice meltwater concentrations. P concentrations were derived using the Redfield ratio C:N:P of 106:6:1 (Redfield, 1958), while keeping N and C concentrations within the range of concentrations detected in GrIS ice melt (Stibal *et al.*, 2012b; Telling *et al.*, 2012; Lawson *et al.*, 2014). Therefore, the experimental set-up provided a realistic scenario for the potential accumulation of organic matter at the surface of glaciers. Nevertheless, the ratio of the organic C:N:P fixed in this experiment was 93:5:1, over one simulated summer, and 90:9:1, over three simulated summers. These ratios are comparable to others reported in cold, high latitude regions (Stibal *et al.*, 2008; Martiny *et al.*, 2013). Cryoconite fertilisation with ambient nutrient conditions (NP and NPC additions) appears to produce a response of self-organisation: P mining out of sediment, autocatalytic N_2 fixation and significant OC fixation. The N_2 fixation was most probably performed by cyanobacteria species belonging to the *Nostocaceae* family, whose

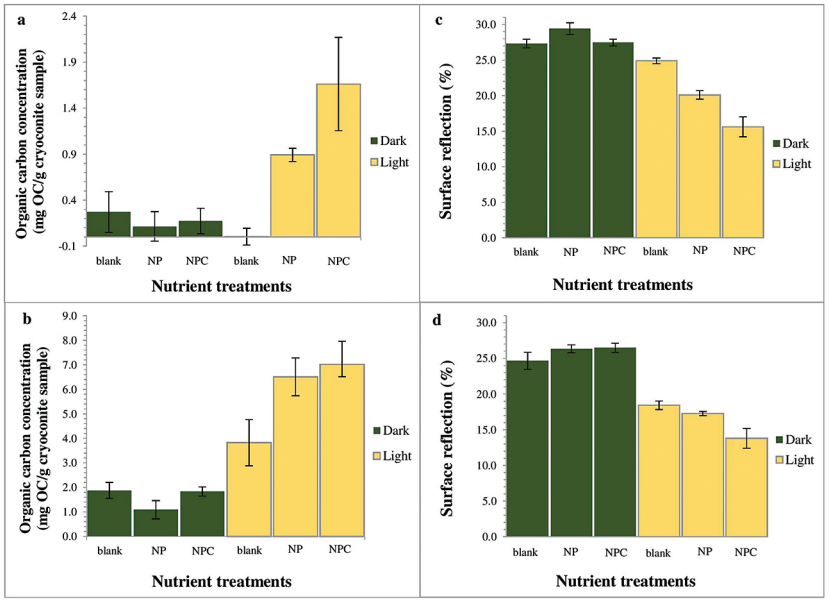

Figure 1 OC accumulated over **(a)** one simulated summer season and **(b)** over three simulated summer seasons. Surface reflection after **(c)** one simulated summer season and **(d)** three simulated summer seasons. 'Light' samples accumulated significantly more OC compared to 'dark' samples (two-way ANOVA $p < 0.05$ in (a) and $p < 0.001$ in (b)). This was accompanied by a decrease in cryoconite sediment reflectivity by ~15.5 percentage points, from a starting 31.1 %, for the 'light' with NPC treatment samples in (c) and a further 1.8 percentage points in (d). Two-way ANOVA analyses showed a significant difference in spectral reflection between 'light' and 'dark' samples ($p < 0.001$), nutrient conditions ($p < 0.001$) and the interaction of nutrient and light settings ($p < 0.01$). There was a significant difference ($p < 0.001$) between samples NPC and blanks, NCP and NP ($p < 0.05$) and NP and blanks ($p < 0.05$), using Turkey Post-hoc analyses in (c-d). Standard errors were calculated as 1σ (n = 5).

16S rRNA and N fixation functional genes have been found within Arctic and Antarctic cryoconite (Cameron *et al.*, 2012a,b). Phosphorous limitation was previously reported in glacial environments (Mindl *et al.*, 2007; Stibal *et al.*, 2009), while N limitation was shown to stimulate N_2 fixation on glaciers (Telling *et al.*, 2011). Supraglacial microbial activity can thus be a vital source of bioavailable nutrients for subglacial and downstream environments.

We hypothesise that adding C as bioavailable carbohydrate, at ambient concentrations, has a kinetic effect on the heterotrophic microbial community, speeding up the recycling of other organic matter. Dependence on labile OC additions demonstrates the importance of heterotrophic processes (recycling nutrients), acting in concert with autotrophic processes (fixing and accumulating OC), in the maintenance of self-organised supraglacial microbial communities. Blank and 'dark' samples receiving no nutrients initially showed no significant

Table 1 Concentrations of PON, OP, IP and chl*a* for each light and nutrient treatment, over one and three simulated summer seasons. The concentrations are the differences between the final and starting concentrations in each treatment. Significant differences (two-way ANOVA) are indicated between **(a)** 'light' and 'dark' samples, **(b)** nutrient treatments and **(c)** the interaction of nutrient and light settings.

Sample conditions		Light			Dark			Two-way ANOVA analysis:
		Sterile water	N and P additions	N, P and C additions	Sterile water	N and P additions	N, P and C additions	
One simulated summer season	PON concentration (µg PON/g cryoconite sample)	11.7 ± 3.8	32.6 ± 21.4	100.4 ± 26.7	-3.1 ± 6.0	-6.6 ± 4.4	-2.4 ± 10.2	**a** ($p < 0.01$)
	OP concentration (µg OC/g cryoconite sample)	-2.1 ± 9.6	13.4 ± 6.0	19.5 ± 6.4	-21.9 ± 1.8	-22 ± 1.7	-10 ± 7.1	**a** ($p < 0.001$) **b** ($p < 0.05$)
	IP concentration (µg OC/g cryoconite sample)	-3.9 ± 5.5	-22 ± 9.8	-27.2 ± 5.4	16.9 ± 8.5	23.6 ± 10.4	12.5 ± 2.4	**a** ($p < 0.001$)
	Chl*a* concentration (in µg of chl*a*/g of sample)	1.6 ± 0.2	3.1 ± 0.1	3.8 ± 0.2	1 ± 0.1	1.1 ± 0.1	1.1 ± 0.0	**a** ($p < 0.001$) **b** ($p < 0.01$) **c** ($p < 0.01$)
Three simulated summer seasons	PON concentration (µg PON/g cryoconite sample)	149.6 ± 31.7	253.4 ± 42.9	680.5 ± 51.1	51.2 ± 19.2	67.3 ± 14.2	61.4 ± 18.1	**a** ($p < 0.001$) **b** ($p < 0.001$) **c** ($p < 0.001$)
	OP concentration (µg OC/g cryoconite sample)	27.7 ± 8.9	35.6 ± 9.1	85.4 ± 13.6	15.2 ± 0.9	13.6 ± 1.4	16.3 ± 4.5	**a** ($p < 0.001$) **b** ($p < 0.001$) **c** ($p < 0.01$)
	IP concentration (µg OC/g cryoconite sample)	-35.6 ± 9.4	-46.7 ± 13.5	-97.7 ± 15.1	-21.8 ± 6.3	-24.1 ± 5.2	-19.6 ± 7.3	**a** ($p < 0.001$) **b** ($p < 0.01$) **c** ($p < 0.01$)
	Chl*a* concentration (in µg of chl*a*/g of sample)	1.5 ± 0.2	2.0 ± 0.0	4.0 ± 0.5	1.0 ± 0.1	1.1 ± 0.2	1.1 ± 0.0	**a** ($p < 0.001$) **b** ($p < 0.001$) **c** ($p < 0.001$)

OC accumulation. However, even these samples showed substantial amounts of OC accumulation after three simulated summer seasons. The blank samples may have simply needed a longer period of time for autotrophic processes to dominate in the microbial community. We postulate that chemolithotrophic activity is the likely explanation for the small OC accumulation in the dark samples.

Impacts of Microbial Activity on Glacial Ice Reflectivity and Calculated Melt Rates. There was a strong negative correlation between OC accumulation and surface reflection (Pearson's $r = -0.897$, $p < 0.05$). The accumulation of microbially-produced OC caused a significant reduction of ~15.5 percentage points in the cryoconite's reflectivity in the 'light' with NPC treatment samples, from a starting 31.1 %, over the one simulated summer (Fig. 1c). It decreased by a further 1.8 percentage points after three simulated summers (Fig. 1d). This is most likely a result of the cryoconite material becoming darker through microbial OC production, accumulation and OC decomposition into dark-coloured humic substances. Microbial activity had the greatest effect in reducing the cryoconite material's surface reflectivity over the first simulated summer. Afterwards, the surface reflectivity of the cryoconite-organic material mixture probably approached a plateau, since further microbial activity and OC accumulation led to only a slight additional reduction in its surface reflectivity after three simulated summers. Additionally, there was a strong correlation between the chl*a* concentration and OC accumulation across all treatments (Table 1, Fig. 1) (Pearson's $r = 0.934$, $p < 0.01$). Cyanobacterial sediment granules only developed in 'light' samples with nutrient additions, after one simulated summer (Fig. 2), which also experienced a substantial decrease in reflectivity. Conversely, blank samples only contained sediment granules after three simulated summers. Furthermore, dark and round microbial cell clusters were predominant in the samples with cyanobacterial granule development. These were most likely colonies of cyanobacteria, such as *Oscillatoriales* and *Nostocales*, previously observed in Greenlandic cryoconite (Cameron *et al.*, 2012b; Stibal *et al.*, 2012b). They may have further contributed to the darkening of the samples' reflectivity. Similar cyanobacterial granules can be found in supraglacial cryoconite holes around the world under *in situ* conditions (Hodson *et al.*, 2010b; Langford *et al.*, 2010). The granules form partially by microbial EPS excretion (Hodson *et al.*, 2010b; Langford *et al.*, 2010), which we suggest enables more nutrient and particle retention within the cryoconite. Further OC fixation and transformation is, therefore, likely to occur in the cryoconite granules, ultimately leading to the darkening of glacial cryoconite sediment. Over longer periods of time, larger cryoconite aggregations will melt into the surface ice to form cryoconite holes, which are more stable environments for organic matter accumulation. However, in the short term, new cryoconite on glaciers undergoes an important decrease in albedo. The increase in anthropogenic NO_3^- deposition on glaciers (Lyons *et al.*, 1990; Duderstadt *et al.*, 2014) has been reported to reduce the microbial N limitation in cryoconite habitats (Telling *et al.*, 2011). Enhanced anthropogenic NO_3^- input will likely lead to a significant decrease in N_2 fixation, allowing more bio-energy to be available for C fixation. Consequently, we envisage that there would be a rise in OC production within cryoconite debris, causing considerable albedo reduction, and thus mass loss on glaciers and ice sheets covered in cryoconite.

We calculated the maximum microbially-mediated GrIS potential melt to be on average 17.3 ± 2.5 Gt yr^{-1}, using the observed 15.5 percentage point decrease in the debris surface reflection (see Methodology, Supplementary Information). This is about 5 % of the present day runoff (Bamber *et al.*, 2012). The estimate is based on a 10 % debris cover concentration, over the extent of GrIS that undergoes persistent melting (more than 1-10 days/yr). The uncertainty in additional melt includes contributions due to the albedo and debris cover, but not any uncertainty in future climate projections. It is, therefore, a first order estimate.

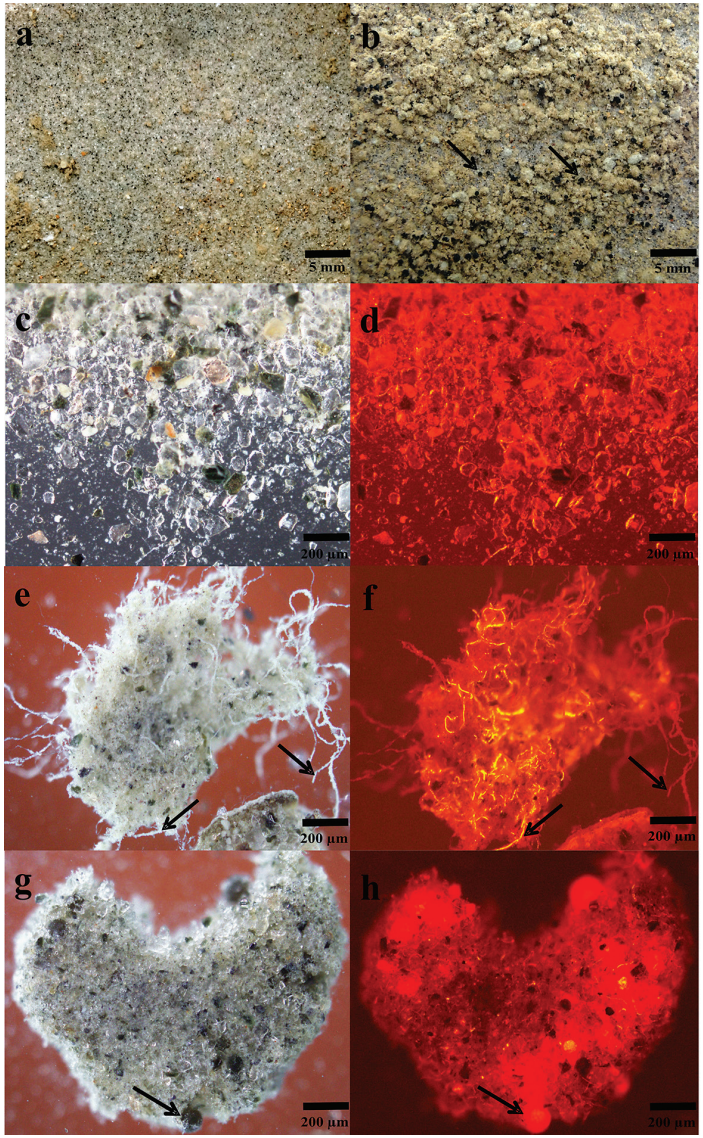

Figure 2 Microbial granule development in 'light' samples with nutrient additions. Images **(a-c)**, **(e)** and **(g)** were taken using optical microscopy. Autofluorescence microscopy was performed to visualise photosynthetic autotrophs in images **(d)**, **(f)** and **(h)**. The initial mixture of inorganic dust with 10 % natural cryoconite (a and c) developed into samples rich in granules and filamentous cyanobacteria (b, e-h). Examples of cyanobacterial filaments and colonies (resembling black spheres) are indicated by arrows in images (b), (e-h).

With the projected changing climate, the GrIS melt area is estimated to expand from the present day 31 % of the total ice sheet (Fig. 3a), to 65 % (Fig. 3b) and 92 % (Fig. 3c) by 2100. These projections are based on two representative greenhouse gas concentration pathways (RCP) 4.5 and 8.5. The former is associated with moderate increases in greenhouse gas concentrations, while the latter is closer to a 'business as usual' trajectory. The effect will be proportionally larger in small Alpine and Arctic valley glaciers, since the melt areas could cover up to 100 % of the glaciers by 2100 (see Methodology, Supplementary Information). The GrIS biologically-induced melt potential could therefore increase up to 42 and 85 Gt yr^{-1}, for RCP 4.5 and 8.5, respectively. These calculations assume no change in NO_3- concentrations and are, therefore, likely a conservative estimate. Furthermore, other ice surface organisms, such as algae (Yallop *et al.*, 2012; Lutz *et al.*, 2014), will likely significantly increase the overall biologically-induced melt potential calculated for cryoconite cyanobacteria in this study. The biological impact on albedo hence plays an important role in modulating mass loss from glacier surfaces and must be included in albedo models to capture adequately the evolving properties of glaciers in a changing climate. Additionally, it is postulated that the warming climate will likely extend melt seasons, leading to increases in biological activity and thus contributing further to the darkening of glaciers and ice sheets (Benning *et al.*, 2014).

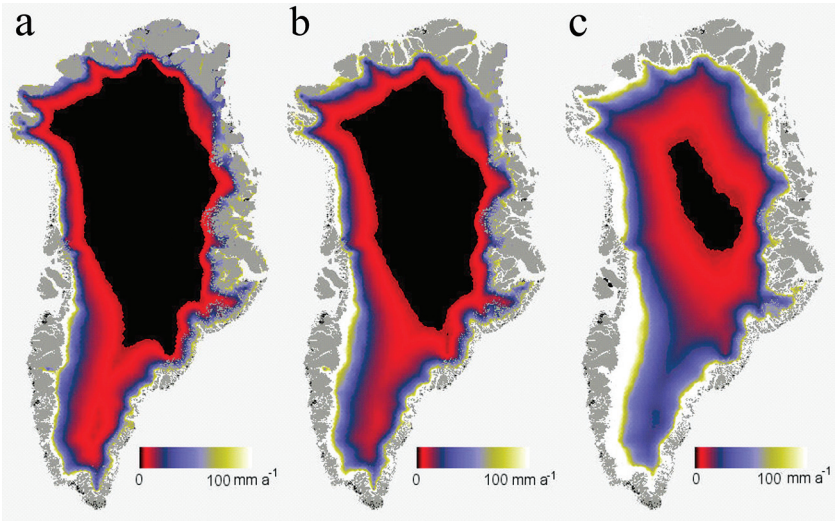

Figure 3 **(a)** Present biologically-induced GrIS potential increase in melt rate, in mm yr^{-1}. **(b)** and **(c)** Future biologically-induced GrIS potential increase in melt rate, in mm yr^{-1}. Melt days were derived for the period 2091-2100 for two different greenhouse gas trajectories, RCP4.5 (b) and RCP8.5 (c).

In conclusion, this study provided for the first time a first-order estimate of the effect of microbial activity on glacial albedo and melt for the GrIS. This effect was significant enough to merit inclusion in albedo models for the GrIS and other glacial environments around the world. In future more elaborate models, other factors (such as the latitudinal variability in PAR; differences between surface reflection and albedo measurements, in the field and in the laboratory; and the influence of surface glacial flow and wind on microbial cryoconite communities) would need to be included to provide a more accurate upscaling of the calculations to the entire GrIS.

Acknowledgements

This study was funded by grants from the UK National Environment Research Council (NERC; NE/J02399X/1 to Anesio and NERC Doctoral Training Programme Grant to Musilova) and the Royal Society International Exchanges Scheme to Anesio and Takeuchi.

Editor: Eric H. Oelkers

Author Contributions

M.M. and A.M.A designed the overall study. M.T. and N.T. were involved in advising the detail of the study design. J.B. performed the climate model simulations. M.M. performed the experiment, collected and processed the data, and wrote the paper. All authors discussed the results and commented on the manuscript.

Additional Information

Supplementary Information accompanies this letter at www.geochemicalperspectivesletters.org/article1611

Cite this letter as: Musilova, M., Tranter, M., Bamber, J.L., Takeuchi, N., Anesio, A.M. (2016) Experimental evidence that microbial activity lowers the albedo of glaciers. *Geochem. Persp. Let.* 2, 106-116.

References

Anesio, A.M., Hodson, A.J., Fritz, A., Psenner, R., Sattler, B. (2009) High microbial activity on glaciers: importance to the global carbon cycle. *Global Change Biology* 15, 955-960.

Bamber, J., van den Broeke, M., Ettema, J., Lenaerts, J., Rignot, E. (2012) Recent large increases in freshwater fluxes from Greenland into the North Atlantic. *Geophysical Research Letters* 39, doi: 10.1029/2012GL052552.

Benning, L.G., Anesio, A.M., Lutz, S., Tranter, M. (2014) Biological impact on Greenland's albedo. *Nature Geoscience* 7, 691-691.

Boggild, C.E., Brandt, R.E., Brown, K.J., Warren, S.G. (2010) The ablation zone in northeast Greenland: ice types, albedos and impurities. *Journal of Glaciology* 56, 101-113.

Box, J.E., Fettweis, X., Stroeve, J.C., Tedesco, M., Hall, D.K., Steffen, K. (2012) Greenland ice sheet albedo feedback: thermodynamics and atmospheric drivers. *Cryosphere* 6, 821-839.

Cameron, K.A., Hodson, A.J., Osborn, A.M. (2012a) Carbon and nitrogen biogeochemical cycling potentials of supraglacial cryoconite communities. *Polar Biology* 35, 1375-1393.

Cameron, K.A., Hodson, A.J., Osborn, A.M. (2012b) Structure and diversity of bacterial, eukaryotic and archaeal communities in glacial cryoconite holes from the Arctic and the Antarctic. *Fems Microbiology Ecology* 82, 254-267.

Doherty, S.J., Grenfell, T.C., Forsstrom, S., Hegg, D.L., Brandt, R.E., Warren, S.G. (2013) Observed vertical redistribution of black carbon and other insoluble light-absorbing particles in melting snow. *Journal of Geophysical Research-Atmospheres* 118, 5553-5569.

Duderstadt, K.A., Dibb, J.E., Jackman, C.H., Randall, C.E., Solomon, S.C., Mills, M.J., Schwadron, N.A., Spence, H.E. (2014) Nitrate deposition to surface snow at Summit, Greenland, following the 9 November 2000 solar proton event. *Journal of Geophysical Research-Atmospheres* 119, 6938-6957.

Dumont, M., Brun, E., Picard, G., Michou, M., Libois, Q., Petit, J.R., Geyer, M., Morin, S., Josse, B. (2014) Contribution of light-absorbing impurities in snow to Greenland's darkening since 2009. *Nature Geoscience* 7, 509-512.

Fettweis, X., Franco, B., Tedesco, M., van Angelen, J.H., Lenaerts, J.T.M., van den Broeke, M.R., Gallee, H. (2013) Estimating the Greenland ice sheet surface mass balance contribution to future sea level rise using the regional atmospheric climate model MAR. *Cryosphere* 7, 469-489.

Fountain, A.G., Tranter, M., Nylen, T.H., Lewis, K.J., Mueller, D.R. (2004) Evolution of cryoconite holes and their contribution to meltwater runoff from glaciers in the McMurdo Dry Valleys, Antarctica. *Journal of Glaciology* 50, 35-45.

Hodson, A., Anesio, A.M., Ng, F., Watson, R., Quirk, J., Irvine-Fynn, T., Dye, A., Clark, C., McCloy, P., Kohler, J., Sattler, B. (2007) A glacier respires: Quantifying the distribution and respiration CO_2 flux of cryoconite across an entire Arctic supraglacial ecosystem. *Journal of Geophysical Research-Biogeosciences* 112, doi: 10.1029/2007JG000452.

Hodson, A., Boggild, C., Hanna, E., Huybrechts, P., Langford, H., Cameron, K., Houldsworth, A. (2010a) The cryoconite ecosystem on the Greenland ice sheet. *Annals of Glaciology* 51, 123-129.

Hodson, A., Cameron, K., Boggild, C., Irvine-Fynn, T., Langford, H., Pearce, D., Banwart, S. (2010b) The structure, biological activity and biogeochemistry of cryoconite aggregates upon an Arctic valley glacier: Longyearbreen, Svalbard. *Journal of Glaciology* 56, 349-362.

Langford, H., Hodson, A., Banwart, S., Boggild, C. (2010) The microstructure and biogeochemistry of Arctic cryoconite granules. *Annals of Glaciology* 51, 87-94.

Lawson, E.C., Wadham, J.L., Tranter, M., Stibal, M., Lis, G.P., Butler, C.E.H., Laybourn-Parry, J., Nienow, P., Chandler, D., Dewsbury, P. (2014) Greenland Ice Sheet exports labile organic carbon to the Arctic oceans. *Biogeosciences* 11, 4015-4028.

Lutz, S., Anesio, A.M., Villar, S.E.J., Benning, L.G. (2014) Variations of algal communities cause darkening of a Greenland glacier. *Fems Microbiology Ecology* 89, 402-414.

Lyons, W.B., Mayewski, P.A., Spencer, M.J., Twickler, M.S. (1990) Nitrate Concentrations in Snow from Remote Areas - Implication for the Global Nox Flux. *Biogeochemistry* 9, 211-222.

Martiny, A.C., Pham, C.T.A., Primeau, F.W., Vrugt, J.A., Moore, J.K., Levin, S.A., Lomas, M.W. (2013) Strong latitudinal patterns in the elemental ratios of marine plankton and organic matter. *Nature Geoscience* 6, 279-283.

Mindl, B., Anesio, A.M., Meirer, K., Hodson, A.J., Laybourn-Parry, J., Sommaruga, R., Sattler, B. (2007) Factors influencing bacterial dynamics along a transect from supraglacial runoff to proglacial lakes of a high Arctic glacier. *Fems Microbiology Ecology* 59, 307-317.

Nakamura, T., Abe, O., Hasegawa, T., Tamura, R., Ohta, T. (2001) Spectral reflectance of snow with a known grain-size distribution in successive metamorphism. *Cold Regions Science and Technology* 32, 13-26.

Paterson, W.S.B. (1994) The physics of glaciers. Elsevier, Oxford, 480 pp.

Pirazzini, R. (2004) Surface albedo measurements over Antarctic sites in summer. *Journal of Geophysical Research-Atmospheres* 109, doi: 10.1029/2004JD004617.

Redfield, A.C. (1958) The Biological Control of Chemical Factors in the Environment. *American Scientist* 46, 205-221.

Ryser, C., Luthi, M., Blindow, N., Suckro, S., Funk, M., Bauder, A. (2013) Cold ice in the ablation zone: Its relation to glacier hydrology and ice water content. *Journal of Geophysical Research-Earth Surface* 118, 693-705.

Stibal, M., Tranter, M., Telling, J., Benning, L.G. (2008) Speciation, phase association and potential bioavailability of phosphorus on a Svalbard glacier. *Biogeochemistry* 90, 1-13.

Stibal, M., Anesio, A.M., Blues, C.J.D., Tranter, M. (2009) Phosphatase activity and organic phosphorus turnover on a high Arctic glacier. *Biogeosciences* 6, 913-922.

Stibal, M., Lawson, E.C., Lis, G.P., Mak, K.M., Wadham, J.L., Anesio, A.M. (2010) Organic matter content and quality in supraglacial debris across the ablation zone of the Greenland ice sheet. *Annals of Glaciology* 51, 1-8.

Stibal, M., Sabacka, M., Zarsky, J. (2012a) Biological processes on glacier and ice sheet surfaces. *Nature Geoscience* 5, 771-774.

Stibal, M., Telling, J., Cook, J., Mak, K.M., Hodson, A., Anesio, A.M. (2012b) Environmental Controls on Microbial Abundance and Activity on the Greenland Ice Sheet: A Multivariate Analysis Approach. *Microbial Ecology* 63, 74-84.

Takeuchi, N., Kohshima, S., Seko, K. (2001) Structure, formation, and darkening process of albedo-reducing material (cryoconite) on a Himalayan glacier: A granular algal mat growing on the glacier. *Arctic Antarctic and Alpine Research* 33, 115-122.

Telling, J., Anesio, A.M., Tranter, M., Irvine-Fynn, T., Hodson, A., Butler, C., Wadham, J. (2011) Nitrogen fixation on Arctic glaciers, Svalbard. *Journal of Geophysical Research-Biogeosciences* 116, doi: 10.1029/2010JG001632.

Telling, J., Stibal, M., Anesio, A.M., Tranter, M., Nias, I., Cook, J., Bellas, C., Lis, G., Wadham, J.L., Sole, A., Nienow, P., Hodson, A. (2012) Microbial nitrogen cycling on the Greenland Ice Sheet. *Biogeosciences* 9, 2431-2442.

Yallop, M.L., Anesio, A.M., Perkins, R.G., Cook, J., Telling, J., Fagan, D., MacFarlane, J., Stibal, M., Barker, G., Bellas, C., Hodson, A., Tranter, M., Wadham, J., Roberts, N.W. (2012) Photophysiology and albedo-changing potential of the ice algal community on the surface of the Greenland ice sheet. *Isme Journal* 6, 2302-2313.

Experimental evidence that microbial activity lowers the albedo of glaciers

M. Musilova[1,2]*, M. Tranter[1], J.L. Bamber[1], N. Takeuchi[3], A.M. Anesio[1]

Supplementary Information

The Supplementary Information includes:

- Methodology
  - Cryoconite Casserole Experimental Setup
  - Nutrient Analysis
  - Surface Reflection
  - Optical and Autofluorescence Microscopy
  - Chlorophyll a (chla) Concentration
  - Calculation of the Impact on the Melt Potential for GrIS
- Supplementary Information References

Methodology

Cryoconite Casserole Experimental Setup

The 'cryoconite casserole' was a laboratory experiment simulating Greenlandic summer glacier surface conditions, in terms of temperature, lighting and nutrient availability achieved with a daylight simulating light rig inside a cold room laboratory. Samples were exposed to ~0 °C underneath the lighting rig. The rig emitted ~105 µmol photons $m^{-2}s^{-1}$ photosynthetically active radiation (PAR) per day for 6 months (20 x Prolite daylight lightbulbs, model: HELIX/30W/BC/640), as measured by a PAR sensor attached to a datalogger (Campbell Scientific CR1000).

1. Bristol Glaciology Centre, School of Geographical Sciences, University of Bristol, Bristol BS8 1SS, UK
2. Current address: Výskumný ústav potravinársky – NPPC and Slovak Organisation for Space Activities (SOSA), Bratislava, Slovakia
* Corresponding author (email: michaela.musilova@community.isunet.edu)
3. Department of Earth Sciences, Graduate School of Science, Chiba University, 1-33, Yayoicho, Inage-ku, Chiba-city, Chiba, 263-8522, Japan

This is the equivalent to the PAR measured over 72 days (268.2 µmol photons $m^{-2}s^{-1}$ PAR per day) in cryoconite holes, throughout one summer season in south-western Greenland (Bagshaw, unpublished data), from where the samples were collected. The lower PAR values used in this experiment, in comparison with the values measured at the sampling site, probably did not substantially influence the microbial activity in the samples, as previous studies have found that incoming solar radiation intensity did not contribute significantly to microbial activity at seasonal time scales (Chandler *et al.*, 2014).

At the start of the simulation, a mixture of Greenlandic cryoconite debris, collected at the surface of Russell Glacier in southwestern Greenland, was added to sterile Pyrex® glass casseroles. The casseroles were previously cleaned 6 x with Milli-Q water (deionised water - 18.2 MΩ cm^{-1}), acid-washed for 48 h and furnaced at 550 °C for 4 h to remove potential traces of OC. The debris was a mixture of 90 % furnaced (550 °C for 4 h) cryoconite material, to remove all organic matter, and 10 % natural cryoconite material. Altogether, 51 g of the mixture were spread on the bottom of each casserole to form a 1 mm layer over 500 cm^2 of the casserole dish. This thin layer of cryoconite simulated the early stages of cryoconite hole development, with mostly inorganic matter present, which can become colonised by microbial communities. The layer was covered by a 1 mm layer of sterile water, which never dried out due to the regular liquid nutrient additions described below. These conditions were similar to those on the surfaces of glaciers, where the freshly deposited cryoconite material generally melts into the surrounding ice. It is thus kept moist for most of the summer season, as well as through regular glacier surface water flow.

Samples were kept either under 'light' (*i.e.* simulated daylight) or 'dark' (*i.e.* covered in aluminium foil) conditions. Phosphorous (P), nitrogen (N) and organic carbon (C) were added to the samples at regular intervals, mimicking nutrient release during ablation on glacier surfaces. N and C were added at concentrations typical of Greenland Ice Sheet (GrIS) ice melt (Stibal *et al.*, 2012; Telling *et al.*, 2012b; Lawson *et al.*, 2014), while the concentration for P was derived using the Redfield ratio C:N:P of 106:6:1 (Redfield, 1958). The nutrients were divided into three different nutrient conditions: 1) blank, sterile water Milli-Q water, 2) N and P additions, and 3) N, P and C additions. The total nutrient concentrations were 0.17 µM KH_2PO_4, 2.72 µM NH_4NO_3 and 18.02 µM $C_6H_{12}O_6$. In total there were 30 samples: 2 light conditions x 3 nutrient conditions x 5 replicates.

Data presented here is from the end of one simulated summer season (*i.e.* after 6 months of laboratory incubation) and after three consecutive summer seasons (*i.e.* after 18 months of incubation). The main purpose of this 18 month experiment was to test for what was observed during the 6 month experiment, *i.e.* whether the microbes inhabiting the cryoconite debris would continue to produce organic matter and thus continue reducing the albedo over longer periods of time. The cryoconite casserole samples were analysed for their nutrient composition, surface reflection, microscopy and chlorophyll *a* concentration, described below.

Nutrient Analyses

Organic carbon. Triplicate cryoconite casserole debris samples were dried at 70 °C for 2 days for total carbon (TC) and nitrogen (TN) analysis on a Eurovector EA3000 Elemental analyser (Telling *et al.*, 2012a). Inorganic carbon (IC) was measured following the same method (Telling *et al.*, 2012a) on a Ströhlein Coulomat 720 analyser. Detection limits for TC, IC and TN were 100 µg C g^{-1} cryoconite, 100 µg C g^{-1} cryoconite and 100 µg N g^{-1} cryoconite, respectively, with an accuracy of ±0.1 %. OC concentration was calculated as the difference between TC and IC (Telling *et al.*, 2012a).

Particulate organic nitrogen. Cryoconite debris-bound exchangeable inorganic NH_4^+, NO_3^- and NO_2^- (whose sum is termed TIN) were extracted using the 2M KCl method modified from Telling *et al.* (2011). The extracts were analysed on a Seal Analytical Autoanalyzer 3, with coefficients of variation for seven replicate standards of 4.8 %, 4.2 %, and 8.7 % for NH_4^+, NO_3^- and NO_2^-, respectively. Detection limits, defined as the sum of the mean of the blanks with 3 x standard deviation (S.D.) of seven Milli-Q water blanks (Telling *et al.*, 2011), were 6.0 µmoles L^{-1}, 1.5 µmoles L^{-1} and 0.2 µmoles L^{-1}, respectively. The debris was weighed after oven drying to convert results to dry weights (Telling *et al.*, 2011). Particulate organic nitrogen (PON) was defined as TN-TIN (Telling *et al.*, 2011), with the TIN extraction recovery considered to be 100 % efficient. Only NH_4^+, NO_3^- and NO_2^- extracts with concentrations above the detection limit were used for the calculations of PON.

Debris-bound phosphorous. The sequential extraction method by Stibal *et al.* (2008) was used to determine the P content associated with five different fractions of dried cryoconite casserole debris ('loosely adsorbed P', 'Fe- and Al-bound' P, 'Ca- and Mg-bound' P, 'organic bound' P and 'inorganic residual' P'). Extracts from the digestions were analysed on a Shimadzu 1240 mini UV-vis spectrophotometer. Only the results from the organic bound P (OP) and inorganic residual P (IP) are presented (see Results and Table 1) for clarity. The residual P represents the remaining IP in the debris after the Ca- and Mg-bound, Fe- and Al-bound and the loosely adsorbed P had been removed during the sequential extractions (Stibal *et al.*, 2008). The detection limits were 0.4 ppm and 0.04 ppm, and the coefficients of variation were 4.8 % and 8.6 % for OP and IP, respectively.

Surface Reflection

An Ocean Optics Jaz modular spectrometer was used to measure the cryoconite surface reflection, as an analogue for albedo. Measurements for reflection were consistently made underneath the lighting rig of the cryoconite casserole experiment, in the same location and at the same height (12 cm perpendicular to the surface of the sample to cover the entire sample surface). Readings were taken at 0.4 nm intervals over a light spectrum range of 339.7–1030.2 nm. Reflection was calculated based on instructions from the manufacturer as:

$$\text{reflection (in \%)} = (\text{sample}_{\text{reflection}} - \text{dark}_{\text{reference}})/(\text{light}_{\text{reference}} - \text{dark}_{\text{reference}}) \times 100 \quad \text{Eq. S-1}$$

where the $dark_{reference}$ was a reflection measurement taken with the optical fibre's light path blocked. The $light_{reference}$ was a reflection measurement taken with the light source on and a blank in the sampling region. A glass casserole dish, on a white reflective panel, was used as the blank to account for any potential additional reflection resulting from the dish itself. The dish had the same amount of liquid as the sample dishes, but no cryoconite debris. Average integration was used for the reflection at visible light wavelengths, in the range of 400-700 nm, to obtain an analogous value for albedo for each sample.

Optical and Autofluorescence Microscopy

Cryoconite casserole samples were collected using sterile spatulas and were spread evenly onto microscopy slides. The structure and composition of the cryoconite sediment was observed with an Olympus BX-51 optical and fluorescent microscope, following previously described methods (Takeuchi *et al.*, 2010). The fluorescence filter used was Olympus U-MWIG3 with excitation and emission (visual) wavelengths of 530-550 µm and >575 µm, respectively.

Chlorophyll a (chla) Concentration

Methods modified from Ameel *et al.* (1998), Stibal *et al.* (2010) and Telling *et al.* (2012a) were used to determine the chl*a* concentration in the cryoconite casserole debris samples, as an estimate of photosynthetic activity. Chl*a* was extracted from 1 g of cryoconite in clean (rinsed 6 x with Milli-Q water and dried) 15 mL centrifuge tubes using 12 mL of ≥99.8 % HPLC grade acetone (CHROMASOLV®), diluted to 90 % using Milli-Q water, in the dark, under nitrogen (Latasa *et al.*, 1996; Szymczak-Żyła *et al.*, 2008) to prevent oxidation. The sample tubes, wrapped in aluminium foil, were shaken on a reciprocating shaker for 30 min at 200 rpm and kept at 4 °C for 24 h (Stibal *et al.*, 2010). Subsequently, the tubes were shaken again for 30 min at 200 rpm and centrifuged at 4000 rpm for 10 min to remove suspended particles, which could interfere with absorbance readings. Remaining pellets in the tubes were dried to determine the dry weight of the debris. The supernatant extracts were analysed by spectrofluorometry on a Fluorolog-3 spectrofluorometer at emission wavelengths of 665 ± 2 nm. Emission values were standardised against purified chl*a* from *Anacystis nidulans* algae (Sigma chemical C6144). Two procedural blanks containing no cryoconite, only 90 % acetone, were run every 10 samples. The detection limit was 3.6 ppb chl*a* and the coefficient of variation was 9.4 %.

Calculation of the Impact on the Melt Potential for GrIS

We assumed a 15.5 % reduction in albedo due to microbial activity within cryoconite (Fig. 1a), scaled up to all GrIS debris cover (as 90 % of microbial activity is associated with the debris; Anesio *et al.*, 2009), over the extent of the ice sheet that experiences persistent melting (more than 1-10 day/yr). We also assumed a

10 % variance in the debris concentration and the albedo reduction in estimating the projected melt uncertainty. While the reduction in spectral reflection was used as a proxy for a reduction in albedo in our calculations and in previous studies (Takeuchi *et al.*, 2001), it is not completely equivalent to albedo, as it does not provide a directional integration of reflectance over all sun-view geometries. The persistent melting of more than 1-10 day/yr was used because the microbial activity within cryoconite is reliant on only a minimal source of liquid water and nutrients, as observed in this experiment. The melt area was determined from the mean of 11 years of satellite passive microwave radiometer observations of daily melt extent for the period 2001-2011 using the XPGR algorithm (Fettweis *et al.*, 2011). Grid cells were only included if they experienced more than 1-10 days melt over the summer. The additional solar radiation absorbed at the surface due the reduction in albedo was calculated from observations of net downwelling shortwave radiation fluxes for JJA near the equilibrium line and ablation zone of the ice sheet (Ettema *et al.*, 2010). This additional energy absorbed was then used to estimate the extra melt at the surface caused by biological activity following the approach detailed by Cawkwell and Bamber (2002). For the projections, we used the global climate model Model for Interdisciplinary Research on Climate (MIROC) CMIP5 output to drive the regional climate model, MAR over Greenland (Fettweis *et al.*, 2013). MIROC lies close to the mid-range response of the CMIP5 simulations over Greenland and is one of a subset that was identified as performing best over the ice sheet (Fettweis *et al.*, 2013). We calculated the change in the number of melt days per grid cell between the mean of 2001-2011 and 2091-2100 for two representative greenhouse gas concentration pathways: RCP 4.5 and RCP 8.5. The present day melt extent from MIROC was scaled to match the present day passive microwave radiometer data (Fig. 3a). For each additional melt day, the increased melting due to a reduction in albedo from biological activity was calculated based on the methods by Cawkwell and Bamber (2002). The 2001-2011 melt days were scaled to match the passive microwave observations for the same period to account for biases in the MIROC simulations (Fettweis *et al.*, 2013). Thus, we were in effect calculating anomalies relative to observed 2001-2011 values (Fig. 3b,c).

The potential melt increase for Alpine and Arctic glaciers was estimated to reach 100 % based on the accumulation area ratio of a glacier (AAR), the percentage of a glacier that remains a snow-covered accumulation zone at the end of the summer melt season. Bahr *et al.* (2009) found an AAR baseline value of 0.57 for worldwide glaciers using long term records, consistent with the study of 24,476 Eurasian glaciers and 5,422 European glaciers (exclusive of Russia) which had an average AAR of 0.58 (Bahr, 1997). The ablation area of these glaciers was therefore 42-43 %. By comparison, the present day GrIS has an AAR of ~0.9 (Ettema, 2010), which corresponds to an ablation area of 10 % and a melt area for the GrIS of 31 % (as calculated above). Assuming that the melt area approximately scales with the ablation area, if the GrIS melt area would increase from 31 % to 65 % or 92 % (RCP 4.5 or RCP 8.5, respectively), then this would mean that the whole of the Alpine and Arctic glaciers would become ablation areas and thus melt areas by 2100.

Supplementary Information References

Ameel, J., Ruzycki, E., Axler, R.P. (1998) Analytical chemistry and quality assurance procedures for natural water samples.*Natural Resources Research Institute technical report*. Central Analytical Laboratory.

Anesio, A.M., Hodson, A.J., Fritz, A., Psenner, R., Sattler, B. (2009) High microbial activity on glaciers: importance to the global carbon cycle. *Global Change Biology* 15, 955-960.

Bahr, D.B. (1997) Width and length scaling of glaciers. *Journal of Glaciology* 43, 557-562.

Bahr, D.B., Dyurgerov, M., Meier, M.F. (2009) Sea-level rise from glaciers and ice caps: A lower bound. *Geophysical Research Letters* 36, doi: doi:10.1029/2008GL036309.

Cawkwell, F.G.L., Bamber, J.L. (2002) The impact of cloud cover on the net radiation budget of the Greenland ice sheet. *Annals of Glaciology*, 34, 141-149.

Chandler, D.M., Alcock, J.D., Wadham, J.L., Mackie, S.L., Telling, J. (2014) Seasonal changes of ice surface characteristics and productivity in the ablation zone of the Greenland Ice Sheet. *Cryosphere* 8, 1337-1382.

Ettema, J. (2010) The present-day climate of Greenland: a study with a regional climate model. PhD Thesis, Utrecht University.

Ettema, J., van den Broeke, M.R., van Meijgaard, E., van de Berg, W.J. (2010) Climate of the Greenland ice sheet using a high-resolution climate model - Part 2: Near-surface climate and energy balance. *Cryosphere* 4, 529-544.

Fettweis, X., Tedesco, M., van den Broeke, M., Ettema, J. (2011) Melting trends over the Greenland ice sheet (1958-2009) from spaceborne microwave data and regional climate models. *Cryosphere* 5, 359-375.

Fettweis, X., Franco, B., Tedesco, M., van Angelen, J.H., Lenaerts, J.T.M., van den Broeke, M.R., Gallee, H. (2013) Estimating the Greenland ice sheet surface mass balance contribution to future sea level rise using the regional atmospheric climate model MAR. *Cryosphere* 7, 469-489.

Latasa, M., Bidigare, R.R., Ondrusek, M.E., Kennicutt, M.C. (1996) HPLC analysis of algal pigments: A comparison exercise among laboratories and recommendations for improved analytical performance. *Marine Chemistry* 51, 315-324.

Lawson, E.C., Wadham, J.L., Tranter, M., Stibal, M., Lis, G.P., Butler, C.E.H., Laybourn-Parry, J., Nienow, P., Chandler, D., Dewsbury, P. (2014) Greenland Ice Sheet exports labile organic carbon to the Arctic oceans. *Biogeosciences* 11, 4015-4028.

Redfield, A.C. (1958) The Biological Control of Chemical Factors in the Environment. *American Scientist* 46, 205-221.

Stibal, M., Tranter, M., Telling, J., Benning, L.G. (2008) Speciation, phase association and potential bioavailability of phosphorus on a Svalbard glacier. *Biogeochemistry* 90, 1-13.

Stibal, M., Lawson, E.C., Lis, G.P., Mak, K.M., Wadham, J.L., Anesio, A.M. (2010) Organic matter content and quality in supraglacial debris across the ablation zone of the Greenland ice sheet. *Annals of Glaciology* 51, 1-8.

Stibal, M., Telling, J., Cook, J., Mak, K.M., Hodson, A., Anesio, A.M. (2012) Environmental Controls on Microbial Abundance and Activity on the Greenland Ice Sheet: A Multivariate Analysis Approach. *Microbial Ecology* 63, 74-84.

Szymczak-Żyła, M., William Louda, J., Kowalewska, G. (2008) Comparison of Extraction and HPLC Methods for Marine Sedimentary Chloropigment Determinations. *Journal of Liquid Chromatography & Related Technologies* 31, 1162-1180.

Takeuchi, N., Kohshima, S., Seko, K. (2001) Structure, formation, and darkening process of albedo-reducing material (cryoconite) on a Himalayan glacier: A granular algal mat growing on the glacier. *Arctic Antarctic and Alpine Research* 33, 115-122.

Takeuchi, N., Nishiyama, H., Li, Z.Q. (2010) Structure and formation process of cryoconite granules on Urumqi glacier No. 1, Tien Shan, China. *Annals of Glaciology* 51, 9-14.

Telling, J., Anesio, A.M., Tranter, M., Irvine-Fynn, T., Hodson, A., Butler, C., Wadham, J. (2011) Nitrogen fixation on Arctic glaciers, Svalbard. *Journal of Geophysical Research-Biogeosciences* 116, doi: 10.1029/2010JG001632.

Telling, J., Anesio, A.M., Tranter, M., Stibal, M., Hawkings, J., Irvine-Fynn, T., Hodson, A., Butler, C., Yallop, M., Wadham, J. (2012a) Controls on the autochthonous production and respiration of organic matter in cryoconite holes on high Arctic glaciers. *Journal of Geophysical Research-Biogeosciences* 117, doi: 10.1029/2011JG001828.

Telling, J., Stibal, M., Anesio, A.M., Tranter, M., Nias, I., Cook, J., Bellas, C., Lis, G., Wadham, J.L., Sole, A., Nienow, P., Hodson, A. (2012b) Microbial nitrogen cycling on the Greenland Ice Sheet. *Biogeosciences* 9, 2431-2442.